

PVLR: Prompt-driven Visual-Linguistic Representation Learning for Multi-Label Image Recognition

Hao Tan^{1,2†}, Zichang Tan^{3†}, Jun Li^{1,2}, Jun Wan^{1,2*}, Zhen Lei^{1,2,4}

¹MAIS, Institute of Automation, Chinese Academy of Sciences, Beijing, China

²School of Artificial Intelligence, University of Chinese Academy of Sciences, Beijing, China

³Department of Computer Vision Technology (VIS), Baidu Inc., Beijing, China

⁴CAIR, HKISI, Chinese Academy of Sciences, Hong Kong, China

{tanhao2023, lijun2021, jun.wan, zhen.lei}@ia.ac.cn, tanzichang@baidu.com

Abstract

Multi-label image recognition is a fundamental task in computer vision. Recently, vision-language models have made notable advancements in this area. However, previous methods often failed to effectively leverage the rich knowledge within language models and instead incorporated label semantics into visual features in a unidirectional manner. In this paper, we propose a **Prompt-driven Visual-Linguistic Representation Learning (PVLR)** framework to better leverage the capabilities of the linguistic modality. In PVLR, we first introduce a dual-prompting strategy comprising Knowledge-Aware Prompting (KAP) and Context-Aware Prompting (CAP). KAP utilizes fixed prompts to capture the intrinsic semantic knowledge and relationships across all labels, while CAP employs learnable prompts to capture context-aware label semantics and relationships. Later, we propose an Interaction and Fusion Module (IFM) to interact and fuse the representations obtained from KAP and CAP. In contrast to the unidirectional fusion in previous works, we introduce a Dual-Modal Attention (DMA) that enables bidirectional interaction between textual and visual features, yielding context-aware label representations and semantic-related visual representations, which are subsequently used to calculate similarities and generate final predictions for all labels. Extensive experiments on three popular datasets including MS-COCO, Pascal VOC 2007, and NUS-WIDE demonstrate the superiority of PVLR.

1. Introduction

Multi-label image classification [5, 6, 8, 13, 21, 23, 26, 33, 34, 37–39, 45–47, 51, 57, 59] is a fundamental task in the field of computer vision, where multiple labels are supposed

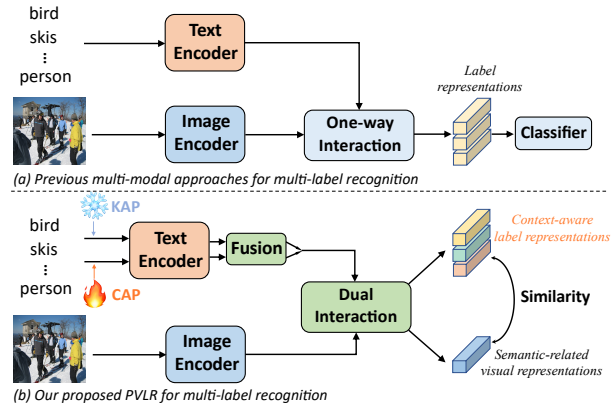


Figure 1. **Paradigm comparison.** (a) Previous methods [6, 38, 47, 57, 59] simply adopt category names to extract text features and they apply a one-way interaction to yield label representations. Then C classifiers are trained to perform recognition. (b) Our method treats the two modalities of equal importance, where we propose dual prompting to extract text features and perform dual interaction to generate context-aware label representations and semantic-related visual representations.

to be recognized in a single image. This ability to capture the diversity of visual content is paramount in applications like image tagging [16, 29], human attribute recognition [35, 36], and recommendation systems [17, 43].

With the rise of vision-language pre-training [18, 31], many approaches [6, 23, 38, 47, 51, 57, 59] have leveraged linguistic modality to mitigate the lack of semantic information from a single visual input. Typically, these approaches involve extracting the inherent semantic knowledge within the language model and employing it as supplementary information to assist the visual model in learning better label representations. Due to the extensive semantic knowledge embedded in language models, these methods have made some improvements in multi-label recognition.

*Corresponding author. † Equal contribution.

However, the application of vision-language modeling in the domain of multi-label image recognition is still in its infancy. One notable limitation is the underutilization of linguistic modality. As summarized in Figure 1, such limitation often manifests in two aspects: **1)** Previous methods [6, 38, 47, 57, 59] simply take the static category names as the inputs of language models (e.g. BERT [10]), which lack sufficient knowledge acquisition and interaction for these powerful models since they are typically pre-trained with complete context (e.g., complete sentences). Such complete context can facilitate the capture of task-relevant semantic information. **2)** The linguistic modality is merely adopted as a supplement of semantic information through a one-way interaction with visual features, which hinders the role of linguistic modality. Thus, C additional classifiers (C is the number of candidate labels) are needed to learn the category centers, which remain static during inference.

In order to address the aforementioned problems, we propose a **Prompt-driven Visual-Linguistic Representation Learning (PVLR)** framework for multi-label image recognition. To tackle the first issue, we propose a dual-prompting strategy, namely **Knowledge-Aware Prompting (KAP)** and **Context-Aware Prompting (CAP)**. Specifically, the recent success of zero-shot predictions [31, 48] by utilizing hand-crafted templates such as “*a photo of a [CLS]*.” motivates us to introduce textual prompts in KAP to facilitate the extraction of general knowledge from language models. However, the KAP remains static and is not informative enough for the vastly changing visual context. Therefore, inspired by recent advancements in prompt learning [52, 53], we further introduce learnable prompts in CAP to facilitate the learning of task-relevant semantics, and adaptively incorporate the visual information into label semantics. To deeply aggregate the information learned by KAP and CAP, we further propose an **Interaction and Fusion Module (IFM)**. The motivation behind the proposed IFM stems from the observation that we humans, when assessing the presence of objects in our surroundings, not only rely on visual information but also employ our prior knowledge to make educated guesses about objects that are partially occluded or viewed from a distant perspective. In this way, we first integrate the knowledge-guided attention map and context-aware attention map generated by KAP and CAP. Then we perform a channel interaction between the label embeddings extracted from KAP and CAP to produce the fused representations for all labels based on the aggregated attention map.

To overcome the second problem, we propose a **Dual-Modal Attention (DMA)** module to treat visual and linguistic modalities of equal importance, which effectively harnesses the advantages of the linguistic modality and captures impactful visual-linguistic representations. Different from existing methods [6, 38, 47, 57, 59] where textual information is only unidirectionally integrated with visual in-

formation, our DMA allows a bidirectional interaction between the two modalities. To achieve this, the proposed DMA consists of two attention modules, i.e., **visual-to-semantic attention** and **semantic-to-visual attention**. Specifically, the visual-to-semantic attention integrates the visual information into the extracted label embeddings, yielding *context-aware label representations*, while the semantic-to-visual attention integrates the extracted label semantics into visual features, resulting in *semantic-related visual representations*. Unlike previous methods [6, 38, 47, 57, 59] that employ fixed classification weights, our method predicts the scores based on the similarity between these two representations, which achieves *input-adaptive category centers*, largely enhancing the model’s generalization capability. To sum up, the main contributions of this work include:

- We propose PVLR, a novel visual-linguistic representation learning framework for multi-label image recognition, which achieves state-of-the-art performance on three widely used benchmarks.
- We emphasize that appropriate prompting can facilitate knowledge extraction from the language model, where we propose KAP and CAP to extract general knowledge and task-relevant semantics respectively. An IFM is further proposed to aggregate their information, which yields powerful prompt-driven label representations.
- Rather than unidirectionally leveraging linguistic information, we propose to perform bidirectional interactions between visual and linguistic modalities, where we generate context-aware label representations and semantic-related visual representations concurrently through DMA, and achieve input-adaptive category centers.

2. Related Work

2.1. Multi-Label Classification

Multi-label recognition serves as a fundamental task in the field of computer vision. Early approaches [5, 21, 37, 39, 45, 46] consider a single visual modality as input and focus on the modeling of label co-occurrence. Some of them rely on the Recurrent Neural Network (RNN) [15] and graph-based models [19]. For example, Wang et al. [37] explored the semantic correlation among labels by cascading the RNN to the feature extractor. Wang et al. [39] utilized the LSTM to capture the dependencies among semantic regions. Ye et al. [46] proposed a dynamic graph convolutional network (GCN) to model the content-aware relations for co-occurred categories. Further works turn to visual attention for implicit relation mining. For instance, Lanchantin et al. [21] utilized a transformer encoder to explore the correlations among visual features and labels. Zhu et al. [55] introduced self-attention to capture spatial relationships and then regularized the predictions. Most recent works further enhance the performance from the per-

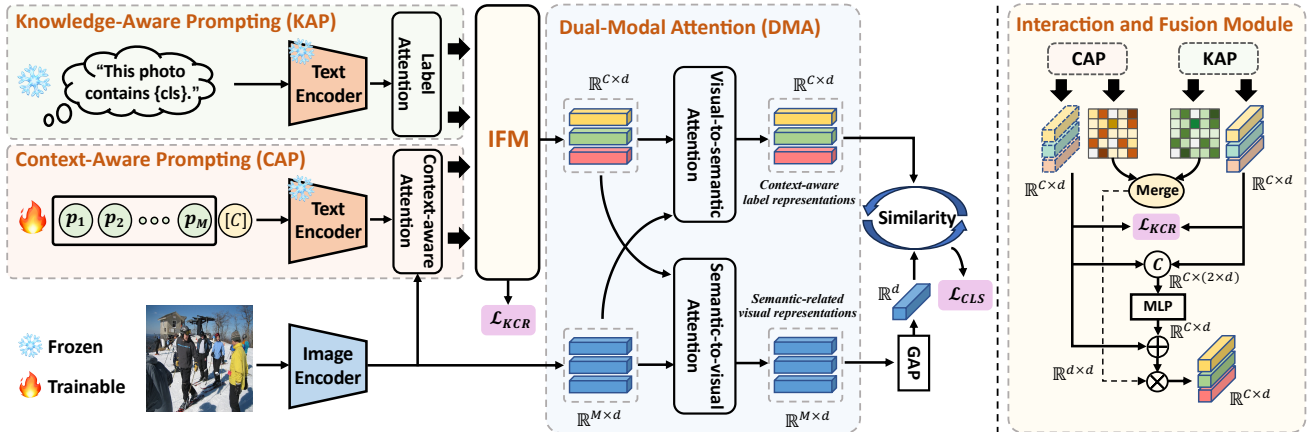


Figure 2. **Overview of the proposed PVLR framework.** 1) KAP adopts fixed prompts to facilitate the extraction of semantic knowledge from the language model. 2) CAP utilizes learnable prompts to integrate context clues into label representations. 3) IFM deeply aggregates the information learned by KAP and CAP through channel interaction. And \mathcal{L}_{KCR} is measured to enhance the generalization. 4) DMA performs bidirectional attention to generate context-aware label representations and semantic-related visual representations, respectively. The context-aware label representations are then regarded as the classification weights and the prediction is based on the similarity between these two representations, which achieves input-adaptive category centers.

spective of knowledge distillation [32, 42] and loss improvements [20]. However, uni-modal methods lack label-related semantic information, which limits their generalization ability. With the rise of language models such as BERT [10], many approaches [6, 8, 23, 26, 38, 47, 51, 57, 59] turn to leveraging linguistic modality to complement the semantic information. Based on the extracted representations for candidate labels, these methods further focus on the interactions of different modalities. You et al. [47] proposed a cross-modality attention module to aggregate visual features and label embeddings, while C classifiers are learned for classification. Similarly, Zhu et al. [57] constructed a two-stream transformer network to explore the textual-visual interactions and an MLP is trained for recognition. Wang et al. [38] superimposed multiple layers of graph to incrementally inject label semantics to feature learning. Chen et al. [6] and Zhu et al. [59] both inserted semantic information to visual features unidirectionally through a low-rank bilinear pooling, while [59] further consider the scene-conditioned label co-occurrence.

Different from them, we explore the mutual interactions between visual and linguistic modality, and further map context-aware label representations into category centers. Although similar approach has appeared in [8], the learning of category centers in their method is agnostic to visual clues. In contrast, the category centers in our work are adaptive to input context, which enhances the generalization.

2.2. Vision-Language Models

Large-scale vision-language pre-training has emerged as a powerful paradigm for a wide range of visual tasks [13,

28, 58]. With a contrastive-based pre-training approach, vision-language models (VLMs) such as CLIP [31] and ALIGN [18] learn a joint representation for visual and linguistic modalities, showing an encouraging ability for efficient transfer learning and zero-shot predictions. More recently, there has been a growing interest in bridging pre-trained LLM and vision foundation models to build VLM. Flamingo [1] introduced gated attention for modality interactions and achieved promising few-shot abilities. BLIP-2 [22] achieved this by training an additional Q-former. While MiniGPT-4 [54] and LLaVA [25] attained impressive multi-modal abilities by only adding a linear projection.

Although previous works have made use of these powerful VLMs, most of them lack sufficient knowledge acquisition from the language model. In contrast, we propose a dual prompting strategy to facilitate the extraction of general knowledge and task-relevant label semantics.

3. Proposed Method

The overall pipeline of our PVLR framework is shown in Figure 2. In this section, we first define some basic notations in Section 3.1, and then introduce the proposed KAP (Section 3.2), CAP (Section 3.3), IFM (Section 3.4) and DMA (Section 3.5) in detail.

3.1. Preliminary

Notations. For multi-label image recognition, assume the input image $I \in \mathbb{R}^{H \times W \times 3}$ is labeled with C candidate categories, where $\mathbf{y} \in \mathbb{R}^C$ represents the multi-hot label vector and $y_j = 1$ means the input image contains the j^{th} label

and vice versa. For the input image I , we employ an image encoder (e.g., ResNet [14] or ViT [11]) to extract visual features $\mathbf{X} \in \mathbb{R}^{M \times d}$, where M indicates the number of pixels or patches, and d is the feature dimension.

Attention mechanism. Transformer has achieved significant success in visual tasks [2, 4, 11], particularly due to its well-designed attention mechanism, which exhibits strong capability in relation modeling. Typically, there are two kinds of attention mechanisms in the transformer, i.e., self-attention and cross-attention. For self-attention, it models the relations among the elements within an input sequence $\mathbf{E} \in \mathbb{R}^{M \times d}$ (M is the number of vectors and d denotes the dimension of the features), which is formulated as:

$$\text{Self-Attn}(\mathbf{E}) = \text{softmax}\left(\frac{\mathbf{Q}\mathbf{K}^\top}{\sqrt{d}}\right)\mathbf{V}, \quad (1)$$

$$\text{where } \mathbf{Q} = \mathbf{E}\mathbf{W}_Q, \mathbf{K} = \mathbf{E}\mathbf{W}_K, \mathbf{V} = \mathbf{E}\mathbf{W}_V,$$

where \mathbf{W}_Q , \mathbf{W}_K and \mathbf{W}_V are learnable weights. We take $\mathcal{M} = \text{softmax}\left(\frac{\mathbf{Q}\mathbf{K}^\top}{\sqrt{d}}\right)$ to denote the attention map that captures the pair-wise relations of vectors in \mathbf{E} . In contrast, cross-attention takes different sources as input and is good at capturing cross-domain interactions. Suppose the inputs are denoted as \mathbf{E} and \mathbf{Z} , the process is formulated as:

$$\text{Cross-Attn}(\mathbf{E}, \mathbf{Z}) = \text{softmax}\left(\frac{\mathbf{Q}\mathbf{K}^\top}{\sqrt{d}}\right)\mathbf{V}, \quad (2)$$

$$\text{where } \mathbf{Q} = \mathbf{E}\mathbf{W}_Q, \mathbf{K} = \mathbf{Z}\mathbf{W}_K, \mathbf{V} = \mathbf{Z}\mathbf{W}_V.$$

3.2. Knowledge-Aware Prompting

Large VLMs [18, 31] typically encompass a wealth of semantic knowledge since the pre-training on large-scale image-text pairs. Therefore, by setting appropriate textual inputs for each label, the embeddings extracted by the language model will contain the underlying semantic relations between different labels.

Hard prompts. Specifically, we take the hand-crafted templates (i.e., hard prompts) “*This photo contains [CLS].*” as the inputs for all C labels. Then the text encoder is adopted to extract C label embeddings, which are denoted as $\mathbf{T}^{hard} = \{\mathbf{t}_1^{hard}, \dots, \mathbf{t}_C^{hard}\} \in \mathbb{R}^{C \times d}$, where d is the hidden dimension of CLIP.

Label attention. Moreover, modeling relations among different labels helps the discovery of the label co-occurrence. Therefore, we perform a label attention on the label embeddings to capture the knowledge-guided relations, which is formally written as:

$$\mathbf{T}^{ka}, \mathcal{M}^{ka} = \text{Self-Attn}(\mathbf{T}^{hard}), \quad (3)$$

where $\mathbf{T}^{ka} \in \mathbb{R}^{C \times d}$ is the relation-enhanced label embeddings. $\mathcal{M}^{ka} \in \mathbb{R}^{C \times C}$ denotes the knowledge-guided attention map, where \mathcal{M}_{ij}^{ka} depicts the relation between \mathbf{t}_i^{hard} and \mathbf{t}_j^{hard} , indicating the underlying co-occurrence probability of the i^{th} and the j^{th} label.

3.3. Context-Aware Prompting

As mentioned above, KAP could extract rich semantic knowledge and relations. However, such information is static and independent of the input image. To address this, we further propose a Context-Aware Prompting (CAP) module to capture context-aware label relations. Compared to KAP, there are mainly two differences in CAP: 1) CAP adopts learnable tokens (i.e., soft prompts) to prompt the language model, which facilitates the learning of downstream semantics, allowing for fine-grained relation exploration. 2) CAP employs a context-aware attention to adaptively aggregate context information into label representations and models the context-aware label relation.

Soft prompts. Inspired by [52, 53], we prepend L prompt tokens to each label and yield “[\mathbf{p}_1][\mathbf{p}_2]...[\mathbf{p}_L][\mathbf{s}_j]”, where $\mathbf{p}_l \in \mathbb{R}^d$ is learnable to adapt the task and \mathbf{s}_j is the word embedding of the j^{th} label name. Then the sequences are fed into text encoder to extract C label embeddings, which are denoted as $\mathbf{T}^{soft} = \{\mathbf{t}_1^{soft}, \dots, \mathbf{t}_C^{soft}\} \in \mathbb{R}^{C \times d}$.

Context-aware attention. To incorporate fine-grained context clues into static label semantics, we condition the label embeddings on visual features, which is formulated as:

$$\begin{aligned} \mathbf{T}'^{soft} &= \text{Cross-Attn}(\mathbf{T}^{soft}, \mathbf{X}), \\ \mathbf{T}^{ca}, \mathcal{M}^{ca} &= \text{Self-Attn}(\mathbf{T}'^{soft}), \end{aligned} \quad (4)$$

where \mathbf{T}'^{soft} captures the interaction between each label representation and all spatial regions. \mathbf{T}^{ca} is the context-aware label representations and \mathcal{M}^{ca} represents the context-aware attention map.

3.4. Interaction and Fusion Module

To fully leverage the strengths of the dual-prompting, we propose an Interaction and Fusion Module (IFM). This consists of two aspects, i.e., the interaction between prompts and the aggregation of relations.

Prompts interaction. To deeply aggregate the information learned by KAP and CAP, we perform an interaction between \mathbf{T}^{ka} and \mathbf{T}^{ca} . Specifically, we propose a channel interaction to continually inject general knowledge to \mathbf{T}^{ca} , which is formulated as:

$$\mathbf{T}^{ca} = \mathbf{T}^{ca} + \text{MLP}([\mathbf{T}^{ka}, \mathbf{T}^{ca}]), \quad (5)$$

where $\text{MLP}(\cdot)$ denotes a Multi-Layer Perceptron and $[\cdot]$ denotes the concatenation operation. For simplicity, we reuse the notation \mathbf{T}^{ca} for the modulated embedding. Moreover, soft prompting is potential to overfit the seen data and forget the general knowledge [3, 44]. Therefore, we further introduce a knowledge-to-context regularization (KCR) loss to enhance the generalization ability, which is formulated as:

$$\mathcal{L}_{KCR} = \frac{1}{C} \sum_{j=1}^C \left(1 - \frac{\mathbf{t}_j^{ka}(\mathbf{t}_j^{ca})^\top}{\|\mathbf{t}_j^{ka}\| \|\mathbf{t}_j^{ca}\|}\right). \quad (6)$$

Relation aggregation. Besides, the relation among labels should consider both general knowledge and practical contexts. Therefore, we propose to aggregate knowledge-guided attention map \mathcal{M}^{ka} and context-aware attention map \mathcal{M}^{ca} through a re-weighting scheme. The aggregated map is then adopted to enhance the label representations:

$$\mathbf{T} = (\alpha\mathcal{M}^{ka} + (1 - \alpha)\mathcal{M}^{ca})\mathbf{T}^{ca}, \quad (7)$$

where α is set to be learnable and $\mathbf{T} \in \mathbb{R}^{C \times d}$ denotes the relation-enhanced label representations.

3.5. Dual-Modal Attention

So far, we have captured the prompt-driven label representations, while the mutual interaction between visual and linguistic modalities is still underexplored. Inspired by [30, 49], we propose to interact visual features and label representations through a dual attention mechanism, which consists of two attention modules, i.e., visual-to-semantic attention and semantic-to-visual attention modules.

Visual-to-semantic attention. To integrate visual information into label representations, we take label representations \mathbf{T} as query and perform a cross-attention with visual features, which is formally written as:

$$\mathbf{T}^{v \rightarrow s} = \text{Cross-Attn}(\mathbf{T}, \mathbf{X}). \quad (8)$$

Semantic-to-visual attention. To inject semantic information into visual representations, we take visual features \mathbf{X} as query and perform a cross-attention with label representations, which is formulated as:

$$\mathbf{X}^{s \rightarrow v} = \text{Cross-Attn}(\mathbf{X}, \mathbf{T}). \quad (9)$$

Then the generated visual features are averaged through a global average pooling (GAP), and we omit the process in the Eq. 9 for simplicity. The acquired label embeddings $\mathbf{T}^{v \rightarrow s} \in \mathbb{R}^{C \times d}$ are aware of visual context and serve as powerful representations for candidate labels. The resulted visual feature $\mathbf{X}^{s \rightarrow v} \in \mathbb{R}^d$ is closely related to the label semantic and is robust to perform final recognition.

Different from previous works [6, 38, 47, 57, 59] that employ fixed classification weights (e.g., linear layers) for recognition, we regard each label representation as the center of the corresponding category, which is an input-adaptive manner and helps to enhance the model’s generalization capability. To be specific, the presence probability of the j^{th} label is predicted through measuring the similarity between visual representation $\mathbf{X}^{s \rightarrow v}$ and the j^{th} label representation $\mathbf{T}_j^{v \rightarrow s}$:

$$\mathbf{p}_j = \sigma(\mathbf{X}^{s \rightarrow v}(\mathbf{T}_j^{v \rightarrow s})^\top), \quad (10)$$

where $\sigma(\cdot)$ is the sigmoid function to map the predicted logit into a probability.

3.6. Training Objective

Based on final predictions in Eq. 10, the Asymmetric Loss [33] is employed for multi-label classification:

$$\mathcal{L}_{CLS} = \frac{1}{C} \sum_{j=1}^C \begin{cases} (1 - \mathbf{p}_j)^{\gamma^+} \log \mathbf{p}_j, & \mathbf{y}_j = 1, \\ \mathbf{p}_j^{\gamma^-} \log(1 - \mathbf{p}_j), & \mathbf{y}_j = 0, \end{cases} \quad (11)$$

where γ^+ and γ^- are asymmetric focusing parameters for positive and negative samples, respectively.

Together with the hard-to-soft regularization loss, the final objective is defined as:

$$\mathcal{L} = \mathcal{L}_{CLS} + \lambda \mathcal{L}_{KCR}, \quad (12)$$

where λ is a hyper-parameter to make a trade-off between the two losses.

4. Experiments

4.1. Datasets and Metrics

MS-COCO. Microsoft COCO [24] is the most widely used dataset to evaluate the task of multi-label classification. It contains 123,287 images in total with 80 categories, where each image has about 2.9 labeled objects. We train the model with training set which contains 82,783 images and evaluate on the test set with 40,504 samples.

PASCAL VOC 2007. VOC 2007 [12] is a popular benchmark for multi-label recognition. It includes 9,963 images in total with 20 distinct object classes. Each image is annotated with 1.4 labels in average. Following [8], we train the model on the *train-val* set which contains 5,011 images and evaluate on the *test set* with 4,952 images.

NUS-WIDE. NUS-WIDE [9] comprises of 269,648 images with a total of 81 visual concepts and 5,018 labels. After filtering out unannotated samples, the training set and test set contain 125,449 and 83,898 images, respectively. Notably, compared with other benchmarks, NUS-WIDE is more noisy and challenging.

Evaluation Metrics. The mean average precision (mAP) is reported to evaluate the overall performance. Following [8, 37, 59], we also report Class-wise Precision (CP), Recall (CR), F1 (CF1), and the average Overall Precision (OP), Recall (OR), F1 (OF1). Note that ‘‘CF1’’ and ‘‘OF1’’ are more informative since Precision and Recall vary with the threshold. To fairly compare with state-of-the-art, we further report top-3 results on MS-COCO and NUS-WIDE.

4.2. Implementation Details

We use CLIP [31] to extract textual embeddings and visual features. Unless specified, the ResNet-101 is used as the image encoder. The text encoder remains frozen in the training phase. The number of learnable prompt tokens L is set to 4. γ^+ and γ^- are set as 0 and 2, respectively. The

Method	Backbone	Resolution	mAP	ALL						Top-3					
				CP	CR	CF1	OP	OR	OF1	CP	CR	CF1	OP	OR	OF1
ML-GCN [8]	ResNet101	(448, 448)	83.0	85.1	72.0	78.0	85.8	75.4	80.3	89.2	64.1	74.6	90.5	66.5	76.7
CMA [47]	ResNet101	(448, 448)	83.4	82.1	73.1	77.3	83.7	76.3	79.9	87.2	64.6	74.2	89.1	66.7	76.3
TSGCN [41]	ResNet101	(448, 448)	83.5	81.5	72.3	76.7	84.9	75.3	79.8	84.1	67.1	74.6	89.5	69.3	69.3
CSRA [56]	ResNet101	(448, 448)	83.5	84.1	72.5	77.9	85.6	75.7	80.3	88.5	64.2	74.4	90.4	66.4	76.5
ASL [33]	ResNet101	(448, 448)	85.0	-	-	80.3	-	-	82.3	-	-	-	-	-	-
TDRL [50]	ResNet101	(448, 448)	84.6	86.0	73.1	79.0	86.6	76.4	81.2	89.9	64.4	75.0	91.2	67.0	77.2
Q2L-R101 [26]	ResNet101	(448, 448)	84.9	84.8	74.5	79.3	86.6	76.9	81.5	78.0	69.1	73.3	80.7	70.6	75.4
SALGL [59]	ResNet101	(448, 448)	85.8	87.2	74.5	80.4	87.8	77.6	82.4	90.4	65.7	76.1	91.9	67.9	78.1
PVLR	ResNet101	(448, 448)	88.2	82.2	82.2	82.2	82.8	85.4	84.1	88.5	69.0	77.6	90.3	71.2	79.6
SSGRL [6]	ResNet101	(576, 576)	83.6	89.5	68.3	76.9	91.2	70.7	79.3	91.9	62.1	73.0	93.6	64.2	76.0
C-Tran [21]	ResNet101	(576, 576)	85.1	86.3	74.3	79.9	87.7	76.5	81.7	90.1	65.7	76.0	92.1	71.4	77.6
ADD-GCN [46]	ResNet101	(576, 576)	85.2	84.7	75.9	80.1	84.9	79.4	82.0	88.8	66.2	75.8	90.3	68.5	77.9
TDRL [50]	ResNet101	(576, 576)	86.0	87.0	74.7	80.1	87.5	77.9	82.4	90.7	65.6	76.2	91.9	68.0	78.1
Q2L-R101 [26]	ResNet101	(576, 576)	86.5	85.8	76.7	81.0	87.0	78.9	82.8	90.4	66.3	76.5	92.4	67.9	78.3
SALGL [59]	ResNet101	(576, 576)	87.3	87.8	76.8	81.9	88.1	79.5	83.6	91.1	66.9	77.2	92.4	69.0	79.0
PVLR	ResNet101	(576, 576)	88.8	82.7	83.1	82.9	83.1	86.1	84.6	88.6	69.6	77.9	90.6	71.5	79.9
M3TR [51]	ViT-B/16	(448, 448)	87.5	88.4	77.2	82.5	88.3	79.8	83.8	91.9	68.1	78.2	92.6	69.6	79.4
PatchCT [23]	ViT-B/16	(448, 448)	88.3	83.3	82.3	82.6	84.2	83.7	83.8	90.7	69.7	78.8	90.3	70.8	79.8
PVLR	ViT-B/16	(448, 448)	90.5	85.1	84.6	84.9	85.1	87.3	86.2	91.1	70.9	79.7	92.0	72.6	81.2

Table 1. **Comparison (%) to state-of-the-art methods on MS-COCO.** Results with different backbone and input resolution are reported. Among them, mAP, OF1, and CF1 are the primary metrics (highlighted in red) as the others may be significantly affected by the threshold.

Method	aero	bike	bird	boat	bottle	bus	car	cat	chair	cow	table	dog	horse	motor	person	plant	sheep	sofa	train	tv	mAP
SSGRL [6]	99.5	97.1	97.6	97.8	82.6	94.8	96.7	98.1	78.0	97.0	85.6	97.8	98.3	96.4	98.8	84.9	96.5	79.8	98.4	92.8	93.4
ML-GCN [8]	99.5	98.5	98.6	98.1	80.8	94.6	97.2	98.2	82.3	95.7	86.4	98.2	98.4	96.7	99.0	84.7	96.7	84.3	98.9	93.7	94.0
TSGCN [41]	98.9	98.5	96.8	97.3	87.5	94.2	97.4	97.7	84.1	92.6	89.3	98.4	98.0	96.1	98.7	84.9	96.6	87.2	98.4	93.7	94.3
ASL [33]	-	-	-	-	-	-	-	-	-	-	-	-	-	-	-	-	-	-	-	-	94.4
CSRA [56]	99.9	98.4	98.1	98.9	82.2	95.3	97.8	97.9	84.6	94.8	90.8	98.1	97.6	96.2	99.1	86.4	95.9	88.3	98.9	94.4	94.7
SALGL [59]	99.9	98.8	98.3	98.2	81.6	96.5	98.1	97.8	85.2	97.0	89.6	98.5	98.7	97.1	99.2	86.9	96.4	89.9	99.5	95.2	95.1
PVLR	99.9	98.1	98.5	98.8	88.8	98.7	97.1	99.4	86.3	98.6	87.4	99.3	98.8	98.5	98.8	85.7	99.4	86.2	98.7	96.0	95.5
Q2L-TRL [26]	99.9	98.9	99.0	98.4	87.7	98.6	98.8	99.1	84.5	98.3	89.2	99.2	99.2	99.2	99.3	90.2	98.8	88.3	99.5	95.5	96.1
M3TR [†] [51]	99.9	99.3	99.1	99.1	84.0	97.6	98.0	99.0	85.9	99.4	93.9	99.5	99.4	98.5	99.2	90.3	99.7	91.6	99.8	96.0	96.5
PatchCT [†] [23]	100.0	99.4	98.8	99.3	87.2	98.6	98.8	99.2	87.2	99.0	95.5	99.4	99.7	98.9	99.1	91.8	99.5	94.5	99.5	96.3	97.1
PVLR[†]	100.0	99.2	99.3	99.4	91.1	99.8	99.0	99.6	90.6	99.4	93.0	99.5	99.4	98.9	99.5	92.1	100.0	91.4	99.3	97.4	97.4

Table 2. **Comparison (%) to state-of-the-art methods on Pascal VOC 2007.** Results are reported in terms of class-wise average precision (AP) and mean average precision (mAP). [†] indicates the ViT-B/16 backbone is used.

hyper-parameter λ is set as 4.0. The input images are resized to 448×448 in both training and testing stages. The network is trained for 30 epochs using AdamW [27] optimizer with a batch size of 64. The learning rate is set as 0.0001 and decays with the cosine policy. Following previous works [33, 59], we apply exponential moving average to model parameters with a decay of 0.9997.

4.3. Comparison with State-of-the-art

The comparisons on MS-COCO, PASCAL VOC 2007, and NUS-WIDE are shown in Table 1, Table 2 and Table 3, respectively. PVLR achieves state-of-the-art performance across various backbones and resolutions on all datasets, surpassing other methods with a decent margin. On the MS-COCO, compared with SALGL [59] that utilized lin-

guistic modality while hindering its role, PVLR exhibits considerable performance gains, exceeding them by 2.4% mAP, suggesting the superiority of fully exploiting linguistic modality. Compared with ML-GCN [8] that also maps label representations into category centers while neglecting the visual context, PVLR achieves 5.2% gains in mAP, demonstrating the effectiveness of learning input-adaptive category centers. Moreover, our method outperforms all other methods on resolution of 576×576 and ViT-B/16 backbone, surpassing previous state-of-the-art by 1.5% and 2.2% mAP respectively. On the NUS-WIDE, our method surpasses all other methods on ResNet101 and ViT-B/16 backbones, achieving 67.4% and 69.0% mAP, respectively, which demonstrates the robustness of PVLR when addressing the noisy real-world images. On the PASCAL VOC

Method	mAP	ALL		Top-3	
		CF1	OF1	CF1	OF1
CMA [47]	61.4	60.5	73.7	55.5	70.0
GM-MLIC [40]	62.2	61.0	74.1	55.3	72.5
ICME [7]	62.8	60.7	74.1	56.3	70.6
ASL [33]	63.9	62.7	74.6	-	-
SALGL [59]	66.3	64.1	75.4	59.5	71.0
PVLR	67.4	65.1	75.5	60.4	71.2
Q2L-TRL [26]	66.3	64.0	75.0	-	-
PatchCT [†] [23]	68.1	65.5	74.7	61.2	71.0
PVLR[†]	69.0	65.6	76.0	62.0	71.7

Table 3. **Comparison (%) to state-of-the-art methods on NUS-WIDE.** [†] indicates ViT-B/16 backbone is used.

KAP	CAP	IFM	DMA	MS-COCO			NUS-WIDE		
				mAP	CF1	OF1	mAP	CF1	OF1
				81.6	54.6	47.7	58.6	29.1	36.6
✓				84.1	78.7	82.1	62.6	57.8	74.8
	✓			86.9	80.4	82.9	65.9	64.0	74.2
✓	✓	✓		87.5	82.0	83.9	66.7	65.2	75.1
✓	✓	✓	✓	88.2	82.2	84.1	67.4	65.1	75.5

Table 4. **Ablation study (%) on the proposed modules.** The baseline method in the first row utilizes the pure category names to extract label representations.

2007, PVLR also outperforms all other methods. With ViT-B/16 backbone, the AP of our method on all 20 categories exceeds 91.1%, which demonstrates the effectiveness of our method in handling objects of distinct sizes and semantics. The experimental results clearly confirm the effectiveness of our proposed method, and also show good generalizability to different network architectures.

4.4. Ablation Studies

Effect of proposed modules. The foremost thing we are interested in is the improvements brought by the proposed KAP, CAP, IFM and DMA. To verify this, we set a baseline method that utilizes pure category names to extract label representations and no further interactions are performed between modalities. As shown in Table 4, the performance of using pure label names is unsatisfactory, leading to poor CF1 and OF1. While KAP heals the performance significantly. We attribute this to that KAP effectively extracts knowledge from the language model. Additionally, applying CAP is extremely effective, improving mAP by 5.3% and 7.3% on MS-COCO and NUS-WIDE respectively. Moreover, employing IFM and DMA can also steadily improve the performance, suggesting that aggregating such static and dynamic information is helpful under the variable visual scenes. These observations fairly verify the effectiveness of our proposed four modules.

Is using label representations as category centers better? In this sub-section, we verify the effectiveness of using

Method	Text	MS-COCO			NUS-WIDE		
		mAP	CF1	OF1	mAP	CF1	OF1
Classifier Learning	CLIP-Text	85.0	78.7	82.4	65.4	63.3	73.3
Label Rep.	CLIP-Text	81.6	54.6	47.7	58.6	29.1	36.6
Label Rep. + DMA	CLIP-Text	87.1	81.3	84.1	65.6	62.6	74.0
PVLR	CLIP-Text	88.2	82.2	84.1	67.4	65.1	75.5
		(↑3.2)	(↑3.5)	(↑1.7)	(↑2.0)	(↑1.8)	(↑2.2)
Classifier Learning	BERT _{Base}	84.8	78.3	82.1	64.8	63.1	73.7
Label Rep.	BERT _{Base}	83.6	78.1	81.8	60.2	57.5	73.6
Label Rep. + DMA	BERT _{Base}	87.3	81.0	83.6	65.9	62.4	74.8
PVLR	BERT _{Base}	88.0	82.2	83.9	66.9	64.7	74.9
		(↑3.2)	(↑3.9)	(↑1.8)	(↑2.1)	(↑1.6)	(↑1.2)

Table 5. **Ablation study (%) on the generation of category centers.** “Label Rep.” means the category centers are generated from label representations.

Method	L	MS-COCO			NUS-WIDE		
		mAP	CF1	OF1	mAP	CF1	OF1
CAP w/ hard prompts	-	87.8	81.7	83.3	66.4	64.2	75.0
CAP w/ pre-interaction	4	87.6	81.9	83.9	65.8	63.7	74.7
CAP w/ soft prompts	4	88.2	82.2	84.1	67.4	65.1	75.5
CAP w/ soft prompts	8	88.2	82.4	84.0	67.0	64.8	75.1
CAP w/ soft prompts	12	88.4	82.3	84.0	66.9	64.6	75.0

Table 6. **Ablation study (%) on the prompting strategy.** L is the number of learnable prompt tokens.

label representations as category centers. Besides our proposed method, we set a “Classifier Learning” experiment as reference, where we perform a one-way interaction and C traditional classifiers are learned (as shown in Figure 1). Accordingly, “Label Rep.” denotes the category centers are mapped from label representations, and “Label Rep. + DMA” indicates that the DMA is further employed. As shown in Table 5, the low performance of “Label Rep.” indicates that generating category centers solely from *static* label representations is inferior, while this can be improved by constructing *dynamic* category centers as “Label Rep. + DMA”. Moreover, PVLR surpasses all three reference methods, which further demonstrates the superiority of our proposed components including KAP, CAP, IFM and DMA. Similar conclusions can be drawn when using BERT [10] as the language model (shown in Table 5).

Effect of prompting strategy. In Table 6, we explore different prompting strategies. Specifically, using hard prompts in CAP yields degraded performance. Conditioning the soft prompts on visual features before the text encoder leads to much more training time and inferior performance (a detailed explanation is provided in the **supplementary material**). Therefore, interacting soft prompts with visual context after the text encoder is a better choice. Moreover, using more prompt tokens (e.g., $L = 8$ or $L = 12$) yields better results on MS-COCO but inferior results on the noisy NUS-WIDE. Therefore, we suggest using 4 prompt tokens in CAP as a good trade-off.

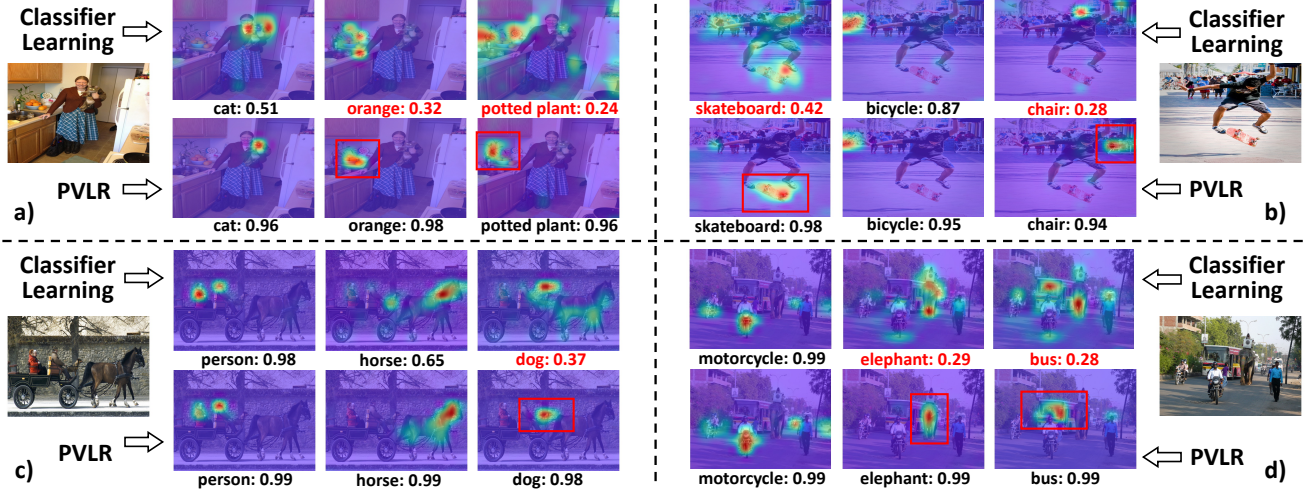


Figure 3. **Visualization of “Classifier Learning” approach and our proposed PVLR.** We present several labels for demonstration and those scores highlighted in **red** are not successfully recognized. PVLR can accurately perceive and localize small objects in a) and b), similar objects in c), and target objects in even complex context in d).

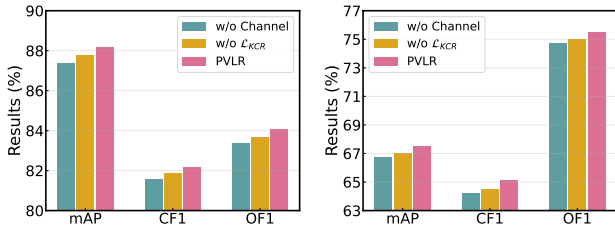


Figure 4. **Ablation study (%) on the IFM.** Results are reported on MS-COCO (left) and NUS-WIDE (right).

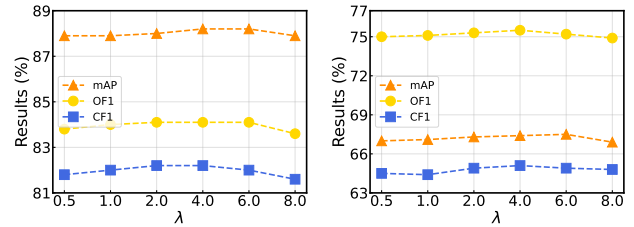


Figure 5. **Sensitivity analysis (%) of λ .** Results are reported on MS-COCO (left) and NUS-WIDE (right).

Components of IFM. As shown in Figure 4, both \mathcal{L}_{KCR} and the channel interaction improve the overall performance, while channel interaction is more important. This indicates that the explicit channel-by-channel interaction is more effective in aggregating the dual prompting branches.

4.5. Further Analyses

Sensitivity analysis of λ . As shown in Figure 5, we evaluate the parameter sensitivity of λ in Eq. 12. The results suggest that the performance of PVLR is generally stable, while $\lambda = 4$ obtains better performance. This indicates the robustness of our method to λ .

Visualization. In Figure 3, we visualize the cross-attention map of the “Classifier Learning” approach and our proposed PVLR. 1) PVLR can more accurately localize small objects, e.g. *orange* in a). 2) PVLR has the ability to distinguish similar objects, e.g. *dog* and *horse* in c) while Classifier Learning confuses them. 3) Classifier Learning exhibits poor capabilities in complex contexts such as d), while PVLR can still precisely localize the target areas. More examples are provided in **supplementary material**.

5. Conclusion

In this work, we propose PVLR, a novel visual-linguistic representation learning framework for multi-label image recognition. To address the defects of existing multi-modal approaches, we propose four modules, namely KAP, CAP, IFM and DMA to fully exploit the linguistic modality and learn the context-aware label representations and semantic-related visual representations concurrently. Extensive experiments show that PVLR achieves state-of-the-art performance on three widely used benchmarks.

Limitations and broader impacts. One limitation is that the semantic knowledge extracted by the pre-trained vision-language model relies on the model’s pretraining data. This may introduce some unexpected noises to our method. Additionally, in our training datasets, there are unannotated objects present in the images, which could impact the model’s performance in real-world scenarios. Our aim in this paper is to develop a general method for multi-label image recognition without targeting specific applications, which does not directly involve specific societal issues.

References

- [1] Jean-Baptiste Alayrac, Jeff Donahue, Pauline Luc, Antoine Miech, Iain Barr, Yana Hasson, Karel Lenc, Arthur Mensch, Katherine Millican, Malcolm Reynolds, et al. Flamingo: a visual language model for few-shot learning. *Advances in Neural Information Processing Systems*, 35:23716–23736, 2022. [3](#)
- [2] Anurag Arnab, Mostafa Dehghani, Georg Heigold, Chen Sun, Mario Lučić, and Cordelia Schmid. Vivit: A video vision transformer. In *Proceedings of the IEEE/CVF international conference on computer vision*, pages 6836–6846, 2021. [4](#)
- [3] Adrian Bulat and Georgios Tzimiropoulos. Lasp: Text-to-text optimization for language-aware soft prompting of vision & language models. In *Proceedings of the IEEE/CVF Conference on Computer Vision and Pattern Recognition*, pages 23232–23241, 2023. [4](#)
- [4] Chun-Fu Richard Chen, Quanfu Fan, and Rameswar Panda. Crossvit: Cross-attention multi-scale vision transformer for image classification. In *Proceedings of the IEEE/CVF international conference on computer vision*, pages 357–366, 2021. [4](#)
- [5] Shang-Fu Chen, Yi-Chen Chen, Chih-Kuan Yeh, and Yu-Chiang Wang. Order-free rnn with visual attention for multi-label classification. In *Proceedings of the AAAI conference on artificial intelligence*, 2018. [1](#), [2](#)
- [6] Tianshui Chen, Muxin Xu, Xiaolu Hui, Hefeng Wu, and Liang Lin. Learning semantic-specific graph representation for multi-label image recognition. In *Proceedings of the IEEE/CVF international conference on computer vision*, pages 522–531, 2019. [1](#), [2](#), [3](#), [5](#), [6](#)
- [7] Zhao-Min Chen, Xiu-Shen Wei, Xin Jin, and Yanwen Guo. Multi-label image recognition with joint class-aware map disentangling and label correlation embedding. In *2019 IEEE International Conference on Multimedia and Expo (ICME)*, pages 622–627. IEEE, 2019. [7](#)
- [8] Zhao-Min Chen, Xiu-Shen Wei, Peng Wang, and Yanwen Guo. Multi-label image recognition with graph convolutional networks. In *Proceedings of the IEEE/CVF conference on computer vision and pattern recognition*, pages 5177–5186, 2019. [1](#), [3](#), [5](#), [6](#)
- [9] Tat-Seng Chua, Jinhui Tang, Richang Hong, Haojie Li, Zhiping Luo, and Yantao Zheng. Nus-wide: a real-world web image database from national university of singapore. In *Proceedings of the ACM international conference on image and video retrieval*, pages 1–9, 2009. [5](#)
- [10] Jacob Devlin, Ming-Wei Chang, Kenton Lee, and Kristina Toutanova. Bert: Pre-training of deep bidirectional transformers for language understanding. *arXiv preprint arXiv:1810.04805*, 2018. [2](#), [3](#), [7](#)
- [11] Alexey Dosovitskiy, Lucas Beyer, Alexander Kolesnikov, Dirk Weissenborn, Xiaohua Zhai, Thomas Unterthiner, Mostafa Dehghani, Matthias Minderer, Georg Heigold, Sylvain Gelly, et al. An image is worth 16x16 words: Transformers for image recognition at scale. *arXiv preprint arXiv:2010.11929*, 2020. [4](#)
- [12] Mark Everingham, Luc Van Gool, Christopher KI Williams, John Winn, and Andrew Zisserman. The pascal visual object classes (voc) challenge. *International journal of computer vision*, 88:303–338, 2010. [5](#)
- [13] Zixian Guo, Bowen Dong, Zhilong Ji, Jinfeng Bai, Yiwen Guo, and Wangmeng Zuo. Texts as images in prompt tuning for multi-label image recognition. In *Proceedings of the IEEE/CVF Conference on Computer Vision and Pattern Recognition*, pages 2808–2817, 2023. [1](#), [3](#)
- [14] Kaiming He, Xiangyu Zhang, Shaoqing Ren, and Jian Sun. Deep residual learning for image recognition. In *Proceedings of the IEEE conference on computer vision and pattern recognition*, pages 770–778, 2016. [4](#)
- [15] Sepp Hochreiter and Jürgen Schmidhuber. Long short-term memory. *Neural computation*, 9(8):1735–1780, 1997. [2](#)
- [16] Xinyu Huang, Youcai Zhang, Jinyu Ma, Weiwei Tian, Rui Feng, Yuejie Zhang, Yaqian Li, Yandong Guo, and Lei Zhang. Tag2text: Guiding vision-language model via image tagging. *arXiv preprint arXiv:2303.05657*, 2023. [1](#)
- [17] Himanshu Jain, Yashoteja Prabhu, and Manik Varma. Extreme multi-label loss functions for recommendation, tagging, ranking & other missing label applications. In *Proceedings of the 22nd ACM SIGKDD international conference on knowledge discovery and data mining*, pages 935–944, 2016. [1](#)
- [18] Chao Jia, Yinfei Yang, Ye Xia, Yi-Ting Chen, Zarana Parekh, Hieu Pham, Quoc Le, Yun-Hsuan Sung, Zhen Li, and Tom Duerig. Scaling up visual and vision-language representation learning with noisy text supervision. In *International conference on machine learning*, pages 4904–4916. PMLR, 2021. [1](#), [3](#), [4](#)
- [19] Thomas N Kipf and Max Welling. Semi-supervised classification with graph convolutional networks. *arXiv preprint arXiv:1609.02907*, 2016. [2](#)
- [20] Takumi Kobayashi. Two-way multi-label loss. In *Proceedings of the IEEE/CVF Conference on Computer Vision and Pattern Recognition*, pages 7476–7485, 2023. [3](#)
- [21] Jack Lanchantin, Tianlu Wang, Vicente Ordonez, and Yanjun Qi. General multi-label image classification with transformers. In *Proceedings of the IEEE/CVF Conference on Computer Vision and Pattern Recognition*, pages 16478–16488, 2021. [1](#), [2](#), [6](#)
- [22] Junnan Li, Dongxu Li, Silvio Savarese, and Steven Hoi. Blip-2: Bootstrapping language-image pre-training with frozen image encoders and large language models. *arXiv preprint arXiv:2301.12597*, 2023. [3](#)
- [23] Miaoge Li, Dongsheng Wang, Xinyang Liu, Zequn Zeng, Ruiying Lu, Bo Chen, and Mingyuan Zhou. Patchct: Aligning patch set and label set with conditional transport for multi-label image classification. In *Proceedings of the IEEE/CVF International Conference on Computer Vision*, pages 15348–15358, 2023. [1](#), [3](#), [6](#), [7](#)
- [24] Tsung-Yi Lin, Michael Maire, Serge Belongie, James Hays, Pietro Perona, Deva Ramanan, Piotr Dollár, and C Lawrence Zitnick. Microsoft coco: Common objects in context. In *Computer Vision–ECCV 2014: 13th European Conference, Zurich, Switzerland, September 6–12, 2014, Proceedings, Part V 13*, pages 740–755. Springer, 2014. [5](#)

- [25] Haotian Liu, Chunyuan Li, Qingyang Wu, and Yong Jae Lee. Visual instruction tuning. *arXiv preprint arXiv:2304.08485*, 2023. [3](#)
- [26] Shilong Liu, Lei Zhang, Xiao Yang, Hang Su, and Jun Zhu. Query2label: A simple transformer way to multi-label classification. *arXiv preprint arXiv:2107.10834*, 2021. [1](#), [3](#), [6](#), [7](#)
- [27] Ilya Loshchilov and Frank Hutter. Decoupled weight decay regularization. *arXiv preprint arXiv:1711.05101*, 2017. [6](#)
- [28] Huaishao Luo, Lei Ji, Ming Zhong, Yang Chen, Wen Lei, Nan Duan, and Tianrui Li. Clip4clip: An empirical study of clip for end to end video clip retrieval and captioning. *Neurocomputing*, 508:293–304, 2022. [3](#)
- [29] Normaisharah Mamat, Mohd Fauzi Othman, Rawad Abdulghafor, Ali A Alwan, and Yonis Gulzar. Enhancing image annotation technique of fruit classification using a deep learning approach. *Sustainability*, 15(2):901, 2023. [1](#)
- [30] Hyeonseob Nam, Jung-Woo Ha, and Jeonghee Kim. Dual attention networks for multimodal reasoning and matching. In *Proceedings of the IEEE conference on computer vision and pattern recognition*, pages 299–307, 2017. [5](#)
- [31] Alec Radford, Jong Wook Kim, Chris Hallacy, Aditya Ramesh, Gabriel Goh, Sandhini Agarwal, Girish Sastry, Amanda Askell, Pamela Mishkin, Jack Clark, et al. Learning transferable visual models from natural language supervision. In *International conference on machine learning*, pages 8748–8763. PMLR, 2021. [1](#), [2](#), [3](#), [4](#), [5](#)
- [32] Sai Rajeswar, Pau Rodriguez, Soumye Singhal, David Vazquez, and Aaron Courville. Multi-label iterated learning for image classification with label ambiguity. In *Proceedings of the IEEE/CVF Conference on Computer Vision and Pattern Recognition*, pages 4783–4793, 2022. [3](#)
- [33] Tal Ridnik, Emanuel Ben-Baruch, Nadav Zamir, Asaf Noy, Itamar Friedman, Matan Protter, and Lihi Zelnik-Manor. Asymmetric loss for multi-label classification. In *Proceedings of the IEEE/CVF International Conference on Computer Vision*, pages 82–91, 2021. [1](#), [5](#), [6](#), [7](#)
- [34] Tal Ridnik, Gilad Sharir, Avi Ben-Cohen, Emanuel Ben-Baruch, and Asaf Noy. MI-decoder: Scalable and versatile classification head. In *Proceedings of the IEEE/CVF Winter Conference on Applications of Computer Vision*, pages 32–41, 2023. [1](#)
- [35] Zichang Tan, Yang Yang, Jun Wan, Hanyuan Hang, Guodong Guo, and Stan Z Li. Attention-based pedestrian attribute analysis. *IEEE transactions on image processing*, 28(12):6126–6140, 2019. [1](#)
- [36] Zichang Tan, Yang Yang, Jun Wan, Guodong Guo, and Stan Z Li. Relation-aware pedestrian attribute recognition with graph convolutional networks. In *Proceedings of the AAAI conference on artificial intelligence*, pages 12055–12062, 2020. [1](#)
- [37] Jiang Wang, Yi Yang, Junhua Mao, Zhiheng Huang, Chang Huang, and Wei Xu. Cnn-rnn: A unified framework for multi-label image classification. In *Proceedings of the IEEE conference on computer vision and pattern recognition*, pages 2285–2294, 2016. [1](#), [2](#), [5](#)
- [38] Ya Wang, Dongliang He, Fu Li, Xiang Long, Zhichao Zhou, Jinwen Ma, and Shilei Wen. Multi-label classification with label graph superimposing. In *Proceedings of the AAAI Conference on Artificial Intelligence*, pages 12265–12272, 2020. [1](#), [2](#), [3](#), [5](#)
- [39] Zhouxia Wang, Tianshui Chen, Guanbin Li, Ruijia Xu, and Liang Lin. Multi-label image recognition by recurrently discovering attentional regions. In *Proceedings of the IEEE international conference on computer vision*, pages 464–472, 2017. [1](#), [2](#)
- [40] Yanan Wu, He Liu, Songhe Feng, Yi Jin, Gengyu Lyu, and Zizhang Wu. Gm-mlc: graph matching based multi-label image classification. *arXiv preprint arXiv:2104.14762*, 2021. [7](#)
- [41] Jiahao Xu, Hongda Tian, Zhiyong Wang, Yang Wang, Wenxiong Kang, and Fang Chen. Joint input and output space learning for multi-label image classification. *IEEE Transactions on Multimedia*, 23:1696–1707, 2020. [6](#)
- [42] Penghui Yang, Ming-Kun Xie, Chen-Chen Zong, Lei Feng, Gang Niu, Masashi Sugiyama, and Sheng-Jun Huang. Multi-label knowledge distillation. In *Proceedings of the IEEE/CVF International Conference on Computer Vision*, pages 17271–17280, 2023. [3](#)
- [43] Xitong Yang, Yuncheng Li, and Jiebo Luo. Pinterest board recommendation for twitter users. In *Proceedings of the 23rd ACM international conference on Multimedia*, pages 963–966, 2015. [1](#)
- [44] Hantao Yao, Rui Zhang, and Changsheng Xu. Visual-language prompt tuning with knowledge-guided context optimization. In *Proceedings of the IEEE/CVF Conference on Computer Vision and Pattern Recognition*, pages 6757–6767, 2023. [4](#)
- [45] Vacit Oguz Yazici, Abel Gonzalez-Garcia, Arnau Ramisa, Bartłomiej Twardowski, and Joost van de Weijer. Orderless recurrent models for multi-label classification. In *Proceedings of the IEEE/CVF Conference on Computer Vision and Pattern Recognition*, pages 13440–13449, 2020. [1](#), [2](#)
- [46] Jin Ye, Junjun He, Xiaojiang Peng, Wenhao Wu, and Yu Qiao. Attention-driven dynamic graph convolutional network for multi-label image recognition. In *Computer Vision—ECCV 2020: 16th European Conference, Glasgow, UK, August 23–28, 2020, Proceedings, Part XXI 16*, pages 649–665. Springer, 2020. [2](#), [6](#)
- [47] Renchun You, Zhiyao Guo, Lei Cui, Xiang Long, Yingze Bao, and Shilei Wen. Cross-modality attention with semantic graph embedding for multi-label classification. In *Proceedings of the AAAI conference on artificial intelligence*, pages 12709–12716, 2020. [1](#), [2](#), [3](#), [5](#), [6](#), [7](#)
- [48] Seonghoon Yu, Paul Hongsuck Seo, and Jeany Son. Zero-shot referring image segmentation with global-local context features. In *Proceedings of the IEEE/CVF Conference on Computer Vision and Pattern Recognition*, pages 19456–19465, 2023. [2](#)
- [49] Lu Yuan, Dongdong Chen, Yi-Ling Chen, Noel Codella, Xiyang Dai, Jianfeng Gao, Houdong Hu, Xuedong Huang, Boxin Li, Chunyuan Li, et al. Florence: A new foundation model for computer vision. *arXiv preprint arXiv:2111.11432*, 2021. [5](#)
- [50] Jiawei Zhao, Ke Yan, Yifan Zhao, Xiaowei Guo, Feiyue Huang, and Jia Li. Transformer-based dual relation graph

- for multi-label image recognition. In *Proceedings of the IEEE/CVF international conference on computer vision*, pages 163–172, 2021. 6
- [51] Jiawei Zhao, Yifan Zhao, and Jia Li. M3tr: Multi-modal multi-label recognition with transformer. In *Proceedings of the 29th ACM international conference on multimedia*, pages 469–477, 2021. 1, 3, 6
- [52] Kaiyang Zhou, Jingkang Yang, Chen Change Loy, and Ziwei Liu. Conditional prompt learning for vision-language models. In *Proceedings of the IEEE/CVF Conference on Computer Vision and Pattern Recognition*, pages 16816–16825, 2022. 2, 4
- [53] Kaiyang Zhou, Jingkang Yang, Chen Change Loy, and Ziwei Liu. Learning to prompt for vision-language models. *International Journal of Computer Vision*, 130(9):2337–2348, 2022. 2, 4
- [54] Deyao Zhu, Jun Chen, Xiaoqian Shen, Xiang Li, and Mohamed Elhoseiny. Minigt-4: Enhancing vision-language understanding with advanced large language models. *arXiv preprint arXiv:2304.10592*, 2023. 3
- [55] Feng Zhu, Hongsheng Li, Wanli Ouyang, Nenghai Yu, and Xiaogang Wang. Learning spatial regularization with image-level supervisions for multi-label image classification. In *Proceedings of the IEEE conference on computer vision and pattern recognition*, pages 5513–5522, 2017. 2
- [56] Ke Zhu and Jianxin Wu. Residual attention: A simple but effective method for multi-label recognition. In *Proceedings of the IEEE/CVF International Conference on Computer Vision*, pages 184–193, 2021. 6
- [57] Xuelin Zhu, Jiuxin Cao, Jiawei Ge, Weijia Liu, and Bo Liu. Two-stream transformer for multi-label image classification. In *Proceedings of the 30th ACM International Conference on Multimedia*, pages 3598–3607, 2022. 1, 2, 3, 5
- [58] Xiangyang Zhu, Renrui Zhang, Bowei He, Ziyao Zeng, Shanghang Zhang, and Peng Gao. Pointclip v2: Adapting clip for powerful 3d open-world learning. *arXiv preprint arXiv:2211.11682*, 2022. 3
- [59] Xuelin Zhu, Jian Liu, Weijia Liu, Jiawei Ge, Bo Liu, and Jiuxin Cao. Scene-aware label graph learning for multi-label image classification. In *Proceedings of the IEEE/CVF International Conference on Computer Vision*, pages 1473–1482, 2023. 1, 2, 3, 5, 6, 7

Appendix

Strategy	Training Speed (seconds/batch)	MS-COCO	NUS-WIDE
Pre-interaction	2.40	87.6	65.8
Post-interaction	0.41	88.2	67.4

Table 7. **Comparison on different strategies in CAP.** The training speed is reported as the training time of a complete forward pass and a backward pass, using a batch size of 64.

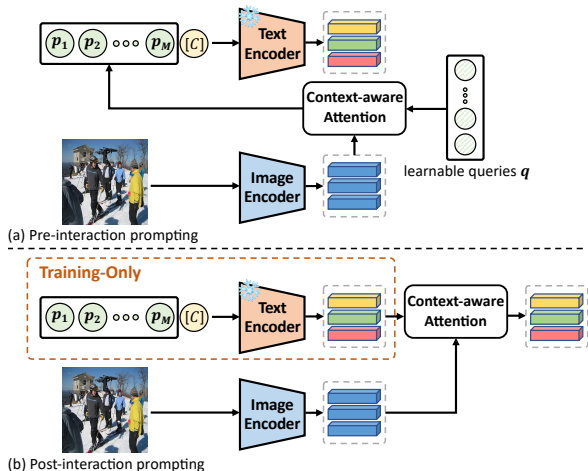


Figure 6. **Different prompting strategies in CAP.**

A. Discussion on Prompting Strategies in CAP

In our proposed CAP, the extracted label embeddings interact with visual features to capture context-aware label semantics. In practice, there are two different strategies to condition the CAP on visual context. As shown in Figure 6, the first is “*pre-interaction prompting*”, where the interaction happens before the text encoder and thus the prompt tokens $\{p_i\}_{i=1}^L$ are generated from the learnable queries and visual features. The second is “*post-interaction prompting*”, where the interaction happens after the text encoder and the label embeddings are refined by the visual features. In this paper, we choose the latter scheme since the former strategy requires an independent forward pass of instance-wise prompts through the text encoder, which consumes significant GPU memory and is less efficient than the latter, while the latter is a lightweight choice and exhibits better performance as reported in Table 7.

B. Discussion on the Bidirectional Interaction

One major distinction of our approach from previous methods is the bidirectional interaction between visual and linguistic modality. In this section, we investigate the effectiveness of the bidirectional interaction. Specifically, our

V-to-S	S-to-V	MS-COCO	NUS-WIDE
		87.5	66.7
✓		87.8	67.0
	✓	87.7	66.2
✓	✓	88.2	67.4

Table 8. **Ablation study (%) on the aggregation of visual clues.** “V-to-S” and “S-to-V” denote visual-to-semantic attention and semantic-to-visual attention, respectively.

Implicit	Explicit	MS-COCO	NUS-WIDE
		86.1	64.8
✓		87.5	66.7
	✓	87.9	66.9
✓	✓	88.2	67.4

Table 9. **Ablation study (%) on the aggregation of visual clues.** PVLR implicitly injects visual information into category centers through CAP, while explicitly incorporating visual information into category centers through DMA.

proposed DMA consists of semantic-to-visual attention and visual-to-semantic attention. By employing only one of them, we perform unidirectional interaction. As shown in Table 8, visual-to-semantic attention steadily improves the mAP, while semantic-to-visual attention hurts the performance on the noisy NUS-WIDE. However, employing both jointly yields significant enhancement, indicating the superiority of bidirectional interaction.

C. Discussion on the Roles of Visual Clues

In PVLR, one core idea is to aggregate visual clues into label representations to yield input-adaptive category centers. In this section, we investigate the effectiveness of such operations. Specifically, we incorporate the visual clues in two aspects. Firstly, we implicitly inject visual information into category centers through CAP. Secondly, we explicitly incorporate visual information into category centers through DMA, which enhances the generalization. The performance is shown in Table 9 by removing either of the two aggregations. Compared to baseline, both implicit and explicit aggregation of visual information improve the mAP significantly, while employing them jointly achieves better results.

D. Additional Results with Different Backbones

We examine our methods on more backbones in Table 10, including ResNet50 and ViT-B/32. Notably, when using a patch size of 32 with ViT-B, the performance is inferior to ResNet101. This may be attributed to that the recognition of some small objects in multi-label images requires more fine-grained visual features. Overall, PVLR achieves

Method	Backbone	MS-COCO			NUS-WIDE		
		mAP	CF1	OF1	mAP	CF1	OF1
PVLR	ResNet50	86.3	80.4	82.5	66.2	63.8	74.9
PVLR	ResNet101	88.2	82.2	84.1	67.4	65.1	75.5
PVLR	ViT-B/32	86.9	80.9	82.6	67.1	64.8	75.5
PVLR	ViT-B/16	90.5	84.9	86.2	69.0	65.6	76.0

Table 10. **Additional results (%) with different backbones.**

steady improvements with more powerful backbones, indicating the generalizability to network architectures.

E. Qualitative Results

In Figure 7, we provide the predicted results of “Classifier Learning” approach and our proposed PVLR with a threshold of 0.5. **1)** Baseline produces many false negative predictions while PVLR mitigates the issue. **2)** Baseline tends to predict “person” in all scenarios, while always neglecting “book” as shown in the last row of Figure 7. We attribute this to that the static category centers in Baseline tend to overfit the distribution of the training set, resulting in high confidence in the frequently occurred labels such as “person”. In contrast, dynamically constructing the context-aware category centers can alleviate this issue.

F. More Visualization Results

In Figure 8, we provide more visualization results of cross-attention maps on MS-COCO. PVLR can accurately perceive and localize objects of distinct sizes and semantics, demonstrating the effectiveness of our method.

	<table border="1"> <thead> <tr> <th>Ground Truth</th> <th>Baseline: CL</th> <th>PVLR</th> </tr> </thead> <tbody> <tr> <td>banana</td> <td>banana</td> <td>banana</td> </tr> <tr> <td>person</td> <td>person</td> <td>person</td> </tr> <tr> <td>motorcycle</td> <td>motorcycle</td> <td>motorcycle</td> </tr> <tr> <td>truck</td> <td>truck</td> <td>truck</td> </tr> </tbody> </table>	Ground Truth	Baseline: CL	PVLR	banana	banana	banana	person	person	person	motorcycle	motorcycle	motorcycle	truck	truck	truck	<table border="1"> <thead> <tr> <th>Ground Truth</th> <th>Baseline: CL</th> <th>PVLR</th> </tr> </thead> <tbody> <tr> <td>mouse</td> <td>mouse</td> <td>mouse</td> </tr> <tr> <td>cell phone</td> <td>person</td> <td>cell phone</td> </tr> <tr> <td>tv</td> <td>keyboard</td> <td>tv</td> </tr> <tr> <td>laptop</td> <td>laptop</td> <td>laptop</td> </tr> <tr> <td></td> <td></td> <td>keyboard</td> </tr> </tbody> </table>	Ground Truth	Baseline: CL	PVLR	mouse	mouse	mouse	cell phone	person	cell phone	tv	keyboard	tv	laptop	laptop	laptop			keyboard												
Ground Truth	Baseline: CL	PVLR																																													
banana	banana	banana																																													
person	person	person																																													
motorcycle	motorcycle	motorcycle																																													
truck	truck	truck																																													
Ground Truth	Baseline: CL	PVLR																																													
mouse	mouse	mouse																																													
cell phone	person	cell phone																																													
tv	keyboard	tv																																													
laptop	laptop	laptop																																													
		keyboard																																													
	<table border="1"> <thead> <tr> <th>Ground Truth</th> <th>Baseline: CL</th> <th>PVLR</th> </tr> </thead> <tbody> <tr> <td>skis</td> <td>skis</td> <td>skis</td> </tr> <tr> <td>person</td> <td>person</td> <td>person</td> </tr> <tr> <td>stop sign</td> <td>stop sign</td> <td>stop sign</td> </tr> </tbody> </table>	Ground Truth	Baseline: CL	PVLR	skis	skis	skis	person	person	person	stop sign	stop sign	stop sign	<table border="1"> <thead> <tr> <th>Ground Truth</th> <th>Baseline: CL</th> <th>PVLR</th> </tr> </thead> <tbody> <tr> <td>microwave</td> <td>microwave</td> <td>microwave</td> </tr> <tr> <td>refrigerator</td> <td>refrigerator</td> <td>refrigerator</td> </tr> <tr> <td>oven</td> <td>oven</td> <td>oven</td> </tr> <tr> <td></td> <td>person</td> <td></td> </tr> </tbody> </table>	Ground Truth	Baseline: CL	PVLR	microwave	microwave	microwave	refrigerator	refrigerator	refrigerator	oven	oven	oven		person																			
Ground Truth	Baseline: CL	PVLR																																													
skis	skis	skis																																													
person	person	person																																													
stop sign	stop sign	stop sign																																													
Ground Truth	Baseline: CL	PVLR																																													
microwave	microwave	microwave																																													
refrigerator	refrigerator	refrigerator																																													
oven	oven	oven																																													
	person																																														
	<table border="1"> <thead> <tr> <th>Ground Truth</th> <th>Baseline: CL</th> <th>PVLR</th> </tr> </thead> <tbody> <tr> <td>person</td> <td>person</td> <td>person</td> </tr> <tr> <td>handbag</td> <td>handbag</td> <td>handbag</td> </tr> <tr> <td>parking meter</td> <td>parking meter</td> <td>parking meter</td> </tr> <tr> <td>truck</td> <td>truck</td> <td>truck</td> </tr> <tr> <td>car</td> <td>car</td> <td>car</td> </tr> </tbody> </table>	Ground Truth	Baseline: CL	PVLR	person	person	person	handbag	handbag	handbag	parking meter	parking meter	parking meter	truck	truck	truck	car	car	car	<table border="1"> <thead> <tr> <th>Ground Truth</th> <th>Baseline: CL</th> <th>PVLR</th> </tr> </thead> <tbody> <tr> <td>person</td> <td>person</td> <td>person</td> </tr> <tr> <td>motorcycle</td> <td>motorcycle</td> <td>motorcycle</td> </tr> <tr> <td>bus</td> <td>bus</td> <td>bus</td> </tr> <tr> <td>elephant</td> <td>elephant</td> <td>elephant</td> </tr> <tr> <td>traffic light</td> <td>traffic light</td> <td>traffic light</td> </tr> <tr> <td>truck</td> <td>truck</td> <td>truck</td> </tr> <tr> <td>car</td> <td>car</td> <td>car</td> </tr> <tr> <td></td> <td>bicycle</td> <td></td> </tr> </tbody> </table>	Ground Truth	Baseline: CL	PVLR	person	person	person	motorcycle	motorcycle	motorcycle	bus	bus	bus	elephant	elephant	elephant	traffic light	traffic light	traffic light	truck	truck	truck	car	car	car		bicycle	
Ground Truth	Baseline: CL	PVLR																																													
person	person	person																																													
handbag	handbag	handbag																																													
parking meter	parking meter	parking meter																																													
truck	truck	truck																																													
car	car	car																																													
Ground Truth	Baseline: CL	PVLR																																													
person	person	person																																													
motorcycle	motorcycle	motorcycle																																													
bus	bus	bus																																													
elephant	elephant	elephant																																													
traffic light	traffic light	traffic light																																													
truck	truck	truck																																													
car	car	car																																													
	bicycle																																														
	<table border="1"> <thead> <tr> <th>Ground Truth</th> <th>Baseline: CL</th> <th>PVLR</th> </tr> </thead> <tbody> <tr> <td>bicycle</td> <td>bicycle</td> <td>bicycle</td> </tr> <tr> <td>person</td> <td>person</td> <td>person</td> </tr> <tr> <td>backpack</td> <td>backpack</td> <td>backpack</td> </tr> </tbody> </table>	Ground Truth	Baseline: CL	PVLR	bicycle	bicycle	bicycle	person	person	person	backpack	backpack	backpack	<table border="1"> <thead> <tr> <th>Ground Truth</th> <th>Baseline: CL</th> <th>PVLR</th> </tr> </thead> <tbody> <tr> <td>person</td> <td>person</td> <td>person</td> </tr> <tr> <td>motorcycle</td> <td>motorcycle</td> <td>motorcycle</td> </tr> <tr> <td>car</td> <td>car</td> <td>car</td> </tr> <tr> <td>truck</td> <td>truck</td> <td>truck</td> </tr> </tbody> </table>	Ground Truth	Baseline: CL	PVLR	person	person	person	motorcycle	motorcycle	motorcycle	car	car	car	truck	truck	truck																		
Ground Truth	Baseline: CL	PVLR																																													
bicycle	bicycle	bicycle																																													
person	person	person																																													
backpack	backpack	backpack																																													
Ground Truth	Baseline: CL	PVLR																																													
person	person	person																																													
motorcycle	motorcycle	motorcycle																																													
car	car	car																																													
truck	truck	truck																																													
	<table border="1"> <thead> <tr> <th>Ground Truth</th> <th>Baseline: CL</th> <th>PVLR</th> </tr> </thead> <tbody> <tr> <td>mouse</td> <td>mouse</td> <td>mouse</td> </tr> <tr> <td>person</td> <td>person</td> <td>person</td> </tr> <tr> <td>tv</td> <td>tv</td> <td>tv</td> </tr> <tr> <td>keyboard</td> <td>keyboard</td> <td>keyboard</td> </tr> <tr> <td>laptop</td> <td>laptop</td> <td>laptop</td> </tr> <tr> <td></td> <td>chair</td> <td>chair</td> </tr> <tr> <td></td> <td></td> <td>handbag</td> </tr> </tbody> </table>	Ground Truth	Baseline: CL	PVLR	mouse	mouse	mouse	person	person	person	tv	tv	tv	keyboard	keyboard	keyboard	laptop	laptop	laptop		chair	chair			handbag	<table border="1"> <thead> <tr> <th>Ground Truth</th> <th>Baseline: CL</th> <th>PVLR</th> </tr> </thead> <tbody> <tr> <td>boat</td> <td>boat</td> <td>boat</td> </tr> <tr> <td>person</td> <td>person</td> <td>person</td> </tr> <tr> <td>car</td> <td>car</td> <td>car</td> </tr> </tbody> </table>	Ground Truth	Baseline: CL	PVLR	boat	boat	boat	person	person	person	car	car	car									
Ground Truth	Baseline: CL	PVLR																																													
mouse	mouse	mouse																																													
person	person	person																																													
tv	tv	tv																																													
keyboard	keyboard	keyboard																																													
laptop	laptop	laptop																																													
	chair	chair																																													
		handbag																																													
Ground Truth	Baseline: CL	PVLR																																													
boat	boat	boat																																													
person	person	person																																													
car	car	car																																													
	<table border="1"> <thead> <tr> <th>Ground Truth</th> <th>Baseline: CL</th> <th>PVLR</th> </tr> </thead> <tbody> <tr> <td>person</td> <td>person</td> <td>person</td> </tr> <tr> <td>elephant</td> <td>elephant</td> <td>elephant</td> </tr> <tr> <td>handbag</td> <td>handbag</td> <td>handbag</td> </tr> </tbody> </table>	Ground Truth	Baseline: CL	PVLR	person	person	person	elephant	elephant	elephant	handbag	handbag	handbag	<table border="1"> <thead> <tr> <th>Ground Truth</th> <th>Baseline: CL</th> <th>PVLR</th> </tr> </thead> <tbody> <tr> <td>person</td> <td>person</td> <td>person</td> </tr> <tr> <td>backpack</td> <td>backpack</td> <td>backpack</td> </tr> <tr> <td>handbag</td> <td>handbag</td> <td>handbag</td> </tr> <tr> <td>traffic light</td> <td>traffic light</td> <td>traffic light</td> </tr> <tr> <td>bus</td> <td>bus</td> <td>bus</td> </tr> <tr> <td>bench</td> <td>bench</td> <td>bench</td> </tr> <tr> <td>cell phone</td> <td>cell phone</td> <td>cell phone</td> </tr> </tbody> </table>	Ground Truth	Baseline: CL	PVLR	person	person	person	backpack	backpack	backpack	handbag	handbag	handbag	traffic light	traffic light	traffic light	bus	bus	bus	bench	bench	bench	cell phone	cell phone	cell phone									
Ground Truth	Baseline: CL	PVLR																																													
person	person	person																																													
elephant	elephant	elephant																																													
handbag	handbag	handbag																																													
Ground Truth	Baseline: CL	PVLR																																													
person	person	person																																													
backpack	backpack	backpack																																													
handbag	handbag	handbag																																													
traffic light	traffic light	traffic light																																													
bus	bus	bus																																													
bench	bench	bench																																													
cell phone	cell phone	cell phone																																													
	<table border="1"> <thead> <tr> <th>Ground Truth</th> <th>Baseline: CL</th> <th>PVLR</th> </tr> </thead> <tbody> <tr> <td>person</td> <td>person</td> <td>person</td> </tr> <tr> <td>clock</td> <td>clock</td> <td>clock</td> </tr> <tr> <td>chair</td> <td>chair</td> <td>chair</td> </tr> <tr> <td>tie</td> <td>tie</td> <td>tie</td> </tr> <tr> <td>book</td> <td>book</td> <td>book</td> </tr> </tbody> </table>	Ground Truth	Baseline: CL	PVLR	person	person	person	clock	clock	clock	chair	chair	chair	tie	tie	tie	book	book	book	<table border="1"> <thead> <tr> <th>Ground Truth</th> <th>Baseline: CL</th> <th>PVLR</th> </tr> </thead> <tbody> <tr> <td>cat</td> <td>cat</td> <td>cat</td> </tr> <tr> <td>chair</td> <td>chair</td> <td>chair</td> </tr> <tr> <td>dining table</td> <td>dining table</td> <td>dining table</td> </tr> <tr> <td>book</td> <td>book</td> <td>book</td> </tr> <tr> <td></td> <td>person</td> <td></td> </tr> </tbody> </table>	Ground Truth	Baseline: CL	PVLR	cat	cat	cat	chair	chair	chair	dining table	dining table	dining table	book	book	book		person										
Ground Truth	Baseline: CL	PVLR																																													
person	person	person																																													
clock	clock	clock																																													
chair	chair	chair																																													
tie	tie	tie																																													
book	book	book																																													
Ground Truth	Baseline: CL	PVLR																																													
cat	cat	cat																																													
chair	chair	chair																																													
dining table	dining table	dining table																																													
book	book	book																																													
	person																																														

Figure 7. Predictions of “Classifier Learning” (CL) baseline and our proposed PVLR. Each sample is marked with three columns. From the left to right are ground truth labels, predictions of baseline and predictions of PVLR, respectively. Correct predictions are marked in **bold** font. Missed objects are highlighted in **blue** and incorrect predictions are marked in **red**. Best viewed in colors.

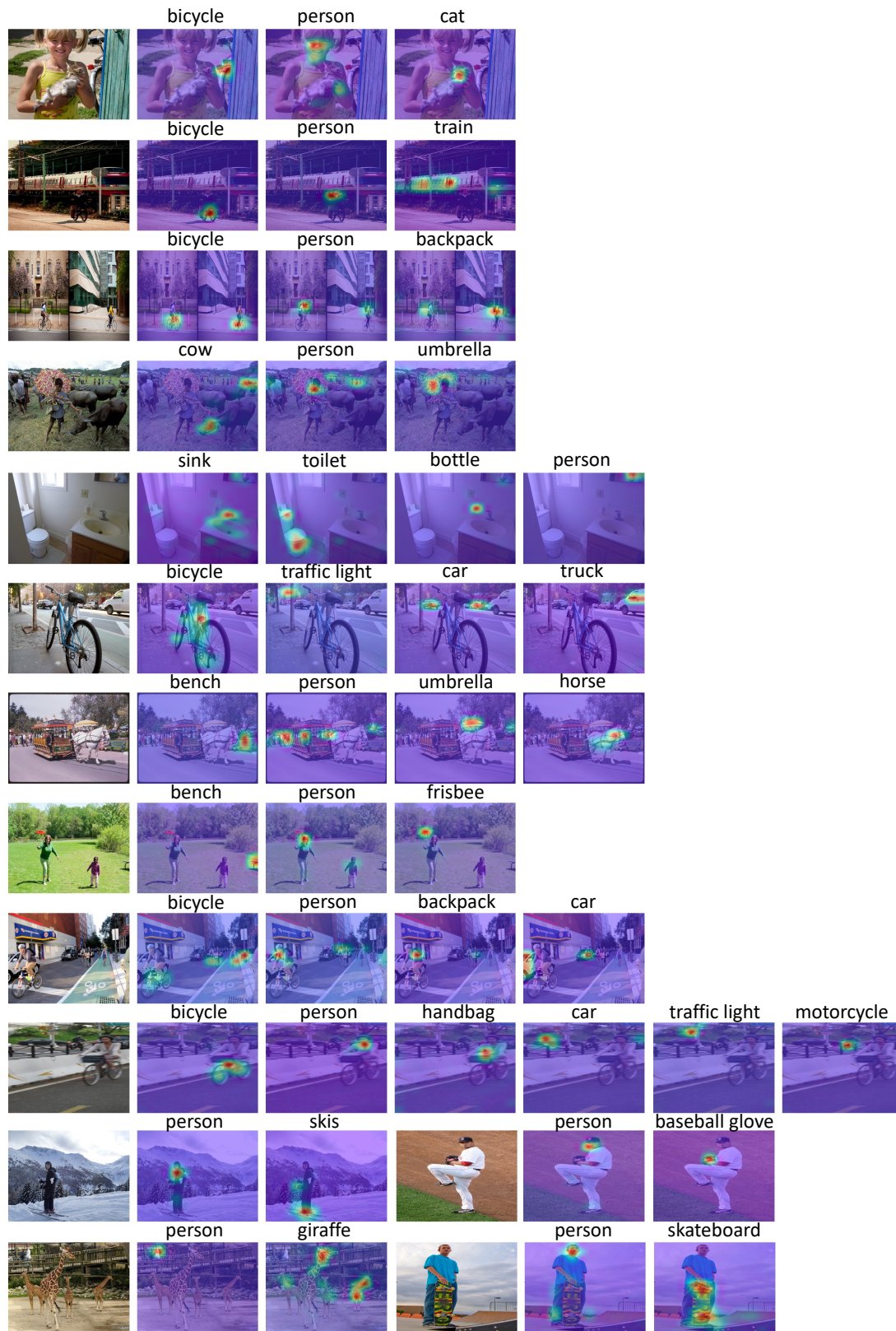


Figure 8. **More visualizations of cross-attention map.** Texts above the images denote the ground truth labels for the images. The brighter the color, the higher the attention to the corresponding area. Best viewed in colors.